Biotechnol. Bioprocess Eng. **2002**, 7: 295-302

Metabolic Flux Analysis of a Poly-β-hydroxybutyrate Producing Cyanobacterium, *Synechococcus* sp. MA19, Grown under Photoautotrophic Conditions

Motomu Nishioka[1], Hajime Nishiuma[1], Masato Miyake[2], Yasuo Asada[3], Kazuyuki Shimizu[4], and Masahito Taya[1]*

[1] Department of Chemical Science and Engineering, Graduate School of Engineering Science, Osaka University, Toyonaka, Osaka 560-8531, Japan
[2] Tissue Engineering Research Center, National Institute of Advanced Industrial Science and Technology, Amagasaki, Hyogo 661-0974, Japan
[3] College of Science and Technology, Nihon University, Funabashi, Chiba 274-8501, Japan
[4] Department of Biochemical Engineering and Science, Kyushu Institute of Technology, Iizuka, Fukuoka 820-0067, Japan

Abstract To understand the utilization property of light energy, *Synechococcus* sp. MA19, a poly-β-hydroxybutyrate (PHB) producer, was cultivated at the different incident light intensities of 15.3, 50.0 and 78.2 W/m^2 using media with and without phosphate. From the results of metabolic flux analysis, it was found that the cell yield based on ATP synthesis was estimated as 3.5×10^{-3} kg-biomass/mol-ATP in these cultures. Under the examined conditions, there were no significant differences in the efficiency of light energy conversion to chemical energies estimated as ATP synthesis and reducing potential (NADH + NADPH) formation whether the PHB synthesis took place or not. The energy converted from light to ATP was kept relatively high around the energy absorbed by the cells of 2.5-3.0 × 10^6 J h^{-1} kg^{-1}, whereas the energy of reducing potential was hardly changed in the examined range of the energy absorbed by the cells.

Keyword: thermophilic cyanobacterium, *Synechococcus* sp., poly-β-hydroxybutyrate, metabolic flux analysis, energy conversion efficiency

INTRODUCTION

The cultures of photosynthetic bacteria offer the potentials for production of useful materials from CO_2. Poly-β-hydroxybutyrate (PHB) is one of the useful and interesting raw materials for biodegradable plastics. Some cyanobactera are known to be capable of producing and accumulating PHB from CO_2 [1,2]. In our previous paper [3], it was reported that thermophilic cyanobacterium, *Synechococcus* sp. MA19, which was isolated from the surface of a wet volcanic rock in Japan [4], could accumulate PHB in the cells up to 55% (w/w) under phosphate-limited conditions.

From a view point of energy capture, photosynthetic bacteria utilize light as a sole energy source and convert the light energy to chemical energy for cell growth and production of metabolites. Recently, intracellular flux analysis has been become of interest as a powerful tool for evaluating metabolic distributions in cells, and applied to many microbial cultures for the purpose of improvement of production processes [5-9]. The knowledge of intracellular flux distributions under different conditions makes it possible to understand the fundamental metabolisms in detail, giving useful information applied to bioreactor designs and control strategies of culture systems. With respect to microalgal cultures, Yang *et al.* [10] employed metabolic flux analysis to discuss the energetics and carbon metabolism of *Chlorella pyrenosidosa* grown under photoautotrophic and mixotrophic conditions. They further reported the carbon flux distributions of *Synechocystis* sp. PCC6803 based on quantitative analysis of intracellular metabolites using gas chromatography/mass spectrometry and two dimensional ^1H-^{13}C correlation nuclear magnetic resonance spectroscopy [11].

In the present study, the photoautotrophic cultures of *Synechococcus* sp. MA19 were conducted using media with and without phosphate. Based on metabolic flux analysis, moreover, the utilization property of light energy was discussed in terms of ATP synthesis and reducing potential (NADH + NADPH) formation.

* **Corresponding author**
Tel: +81-6-6850-6251 Fax: +81-6-6850-6254
e-mail: taya@cheng.es.osaka-u.ac.jp

MATERIALS AND METHODS

Bacterial Culture and Medium

A thermophilic PHB-producing cyanobacterium,

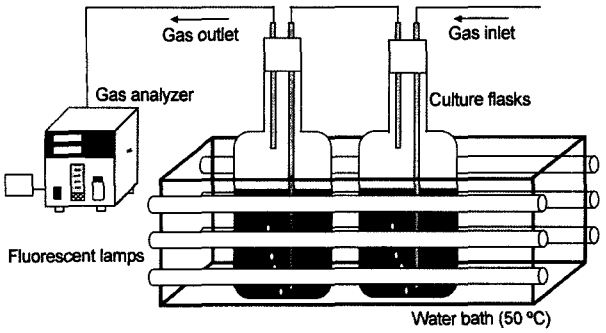

Fig. 1. Setup of equipment for cultivation of *Synechococcus* sp. MA19 under photoautotrophic conditions.

Synechococcus sp. MA19 [4], was cultivated in a BG11 basal medium [12] containing 1.5 g $NaNO_3$, 30 mg K_2HPO_4, 75 mg $MgSO_4 \cdot 7H_2O$, 35 mg $CaCl_2 \cdot 2H_2O$, 6 mg citric acid, 6 mg ferric ammonium citrate, 1 mg EDTA· 2Na, 1 mg Na_2CO_3, 2.86 mg H_3BO_4, 0.222 mg $CuSO_4 \cdot 5H_2O$, 0.021 mg $Na_2MoO_4 \cdot 2H_2O$, 10 mg vitamin B_{12}, and 11.9 g HEPES (Dojindo Lab., Kumamoto, Japan) in 1 dm^3 of distilled water. The medium pH was adjusted to 8 with NaOH solution. When phosphate-free BG11 medium was used, K_2HPO_4 was omitted from the medium components. Each culture started with 10% (v/v) inoculum. The cells were grown at 50 °C in a couple of 2 dm^3 flat, oblong flasks (16 cm wide × 40 cm high × 4 cm deep) connected in series (working volume of each flask, $V = 1.8 \times 10^{-3}$ m^3), as shown in Fig. 1. The culture was illuminated at both sides of the flasks with a bank of fluorescent lamps at an incident light intensity, I_0, of 15.3, 50.0, or 78.2 W/m^2. Air containing 2% (v/v) CO_2 was introduced into the flasks at a flow rate of 50 cm^3/min.

Analytical Methods

The concentration of cell mass, X, and PHB content in the cells, R_P, were determined by the methods described elsewhere [3]. The amount of cellular components besides PHB, X_C, calculated by $X_C = X(1\text{-}R_P)$, was recorded as biomass in the present study. Partial pressures of CO_2 and O_2 in the flowing gas phase were measured using a gas analyzer (Model DEX-1562-1, ABLE, Japan), and CO_2 uptake rate, *CUR*, and O_2 evolution rate, *OER*, during the cultures were estimated based on the gas flow rate and partial pressures of CO_2 and O_2 in inlet and outlet gas phases. Incident light intensity, I_0, was measured by using an illuminometer (Model M-10A2, ABLE, Japan). Light energy absorbed in the cell suspension, E_C, was calculated according to the method described elsewhere [13]. The light attenuation through absorption by the cells was expressed based on a Lambert-Beer formula with effective absorption coefficient, α, and total light energy absorbed in the cell suspension, E_T, was calculated by the following equation, taking account of light irradiation on the both side faces of each flask.

$$E_T = 2 \cdot (3600)\, I_0 A\{1\text{-}\exp(-\alpha(X) \cdot L)\} \quad (1)$$

where $A = 6.4 \times 10^{-2}$ m^2 and $L = 0.04$ m in the present study. The α value was determined from the data of the light transmittance against light path length measured at various cell concentrations, and was correlated with the X value by the empirical equation as follows.

$$\alpha(X) = 38X^{0.38} + 7.0 \quad (2)$$

Then, net light energy absorbed by the cells was determined as follows.

$$E_C = (E_T\text{-}E_M)/XV \quad (3)$$

Hence the value of E_M was obtained by substituting α = 7.0 m^{-1} (determined from light transmittance in the cell-free medium) for Eq. (1).

Metabolic Flux Analysis

Metabolic Network of Synechococcus *sp. MA19 Cells*

The central metabolic network in MA19 cells grown under a photoautotrophic condition was constructed according to those of other microbes found in the publications [6,9,14]. The genomic information of *Synechocystis* sp. PCC6803 (CyanoBase, URL: http://www.kazusa.or.jp/cyano/, March 10, 2001) was employed for reference of enzymatic reactions involved in metabolic fluxes of MA19 cells. CO_2 is fixed through photosynthesis (Calvin-Benson cycle), incorporated into glycolysis in a form of phosphoglycerate (PGA), and metabolized through tricarboxylic acid pathway, associated with PHB synthesis via acetyl-CoA under a phosphate-limited conditions [3]. As ATP-forming pathways, oxidative phosphorylation and photophosphorylation were included in the network. Calvin-Benson cycle and pentose phosphate pathway sharing their intermediates were combined into one pathway for convenience in the present study.

Flux Calculation in Metabolic Network

A stoichiometric model combined with measurements of substrate and extracellular products was applied to the estimation of intracellular metabolite fluxes. The metabolite accumulation rates can be expressed as follows.

$$\boldsymbol{r}_{ij} = \Sigma\, a_{ij}\boldsymbol{x}_j \quad (i = 1, 2, \ldots, m, \text{ and } j = 1, 2, \ldots, n) \quad (4)$$

where $\boldsymbol{r}_{ij}$ is the accumulation rate of a metabolite i, a_{ij} a stoichiometric coefficient and $\boldsymbol{x}_j$ the flux through jth reaction. The metabolite i and reaction j involved in the metabolic network in MA19 cells are specified in Appendices A and B, respectively. Based on the mass balances of respective metabolites, the following equation can be obtained.

$$\boldsymbol{S}\boldsymbol{x} = \boldsymbol{r} \quad (5)$$

where $\boldsymbol{S}$ is $m \times n$ matrix of stoichiometric coefficients, $\boldsymbol{x}$ an n-dimensional flux vector, and $\boldsymbol{r}$ an m-dimensional metabolite accumulation vector. The weighted least square solution to Eq. (5), provided $m \geq n$ and $\boldsymbol{S}$ is of full rank, is

$$\boldsymbol{x} = (\boldsymbol{S}^T\varphi^{-1}\boldsymbol{S})^{-1}\boldsymbol{S}^T\varphi^{-1}\boldsymbol{r} \quad (6)$$

where φ is the matrix of measurement noise variance-covariance with respect to the vector $\boldsymbol{r}$.

The elements of $\boldsymbol{r}$ considered in the present study are given in Appendix A, where the measured extracellular compounds are cell mass including biomass (cellular components) and PHB fractions, CO_2 and O_2, because usual metabolites such as organic acids and ethanol are not formed as end products by MA19 cells. The elements of $\boldsymbol{r}$ corresponding intracellular metabolites were set to zero by approximating a pseudo-steady-state for concentration of intracellular metabolites according to the literature [15]. The diagonal elements of φ were calculated from the variance of measured data for the extracellular compounds, where standard deviations of the measurement data were 5% for the amounts of cell mass and PHB, and 10% for the *CUR* and *OER* values. Variance for intracellular metabolites was set to zero.

Biomass synthesis was represented as a lump equation, where stoichiometric coefficients were determined from composition of major cellular components so as to match the elemental formula of $C_4H_7N_{0.89}O_{1.48}$ (with 9.22% ash), which was obtained experimentally for biomass fraction of MA19 cells excluding PHB, according to the literatures [15-18]. A reaction was also included for dissipating excess ATP for maintenance metabolism, transport costs, or the energies required to retain concentration gradients across cell membranes.

To handle an ill-posed problem due to rank efficiency, the following two equations were assumed in the present study.

1) According to the previous study (14), photosynthetic CO_2 fixation rate is equivalent to photosynthetic O_2 evolution rate, so that the following equation holds:

$$x_{15} = x_{16} \quad (7)$$

where x_{15} and x_{16} are the fluxes of photosynthetic O_2 evolution and photosynthetic CO_2 fixation, respectively (Appendix B).

2) Actual O_2 evolution rate, r_o, depends on light energy absorbed by the cells, E_C. Fig. 2 shows the relation between the r_o and E_C values, which were determined in a series of measurements using conducted MA19 cells cultures under various light conditions. The following empirical equation was then obtained from the data matching by the nonlinear least-squares method.

$$r_o = 1.74E_C / (3.55\times10^5 + E_C) - 0.488 \quad (8)$$

Employing Eqs. (7) and (8), the matrix A is of full rank and the flux distribution could be calculated using a software, BIONET [6].

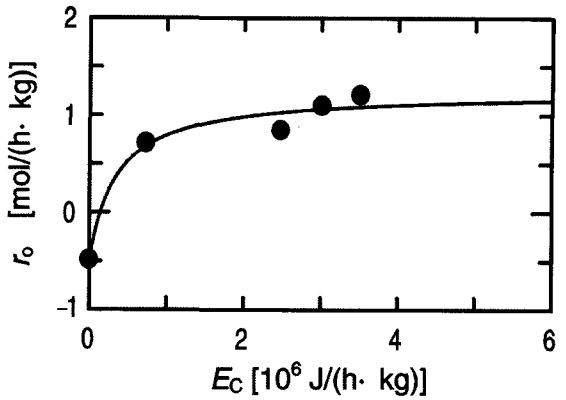

Fig. 2. Relationship between r_o and E_C values determined for *Synechococcus* sp. MA19 cells. The line was fitted by Eq. (8).

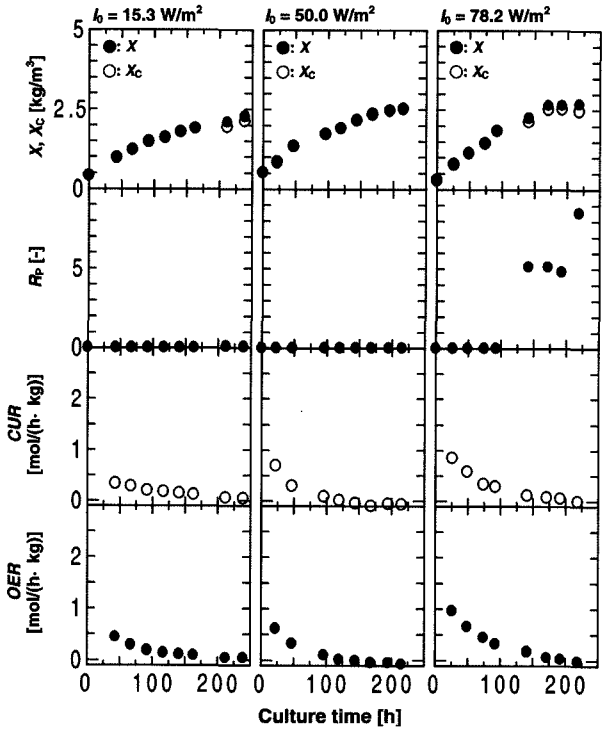

Fig. 3. Time profiles of *Synechococcus* sp. MA19 cultures in phosphate-containing medium at different incident light intensities of 15.3, 50.0 and 78.2 W/m².

RESULTS AND DISCUSSION

Batch Cultures of *Synechococcus* sp. MA19 in Media with and without Phosphate

In the previous study [3], it was reported that phosphate in the medium was one of the key factors to induce the accumulation of PHB in MA19 cells. In the pre-

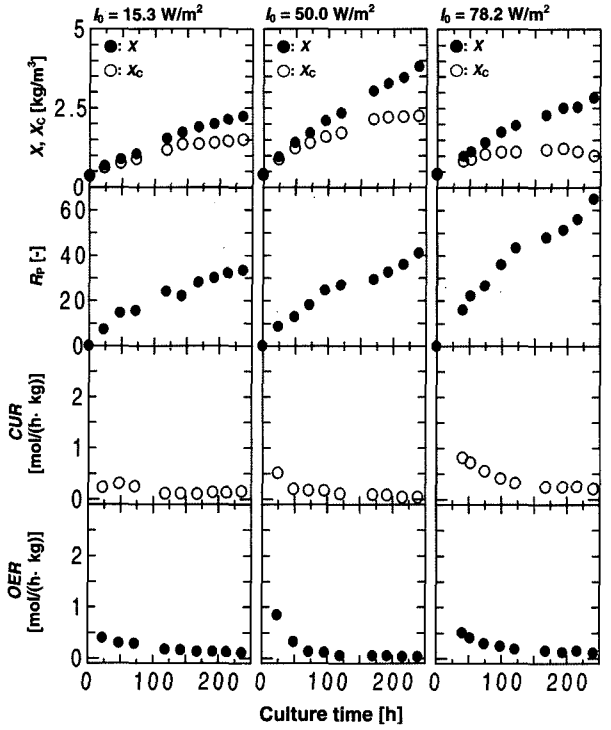

Fig. 4. Time profiles of *Synechococcus* sp. MA19 cultures in phosphate-free medium at different incident light intensities of 15.3, 50.0 and 78.2 W/m^2.

sent work, the batch cultures of MA19 cells were then conducted using phosphate-containing BG11 and phosphate-free BG11 media under the photoautotrophic conditions at incident light intensities of 15.3, 50.0, and 78.2 W/m^2. In the cultures using the medium with phosphate as shown in Fig. 3, notable PHB accumulation was not observed at the examined incident light intensities. These results indicated that the phosphate limitation did not take place for the production of PHB in MA19 cells cultivated under the examined conditions (phosphate concentration in medium: 0.027-0.17 mol/m^3, estimated from cell yield on a phosphate basis). The amount of cellular components, X_C, was increased with elapsed time of culture and reached almost the same level at the end of cultures (X_C = 2.3, 2.5 and 2.5 kg/m^3 at I_0 = 15.3, 50.0 and 78.2 W/m^2 respectively). In any cultures, the growth of MA19 cells was retarded at the late periods of cultures, values of *CUR* and *OER* approaching zero.

On the other hand, in the cultures using the phosphate-free medium, the increases in X_C value stopped during the relatively early stages of cultures in the three intensities of incident light (Fig. 4). To the contrary, PHB accumulation started at the early periods of cultures under any light conditions and the value of PHB content, R_P, increased as light intensity increased. Phosphate was not detected in the medium throughout these cultures.

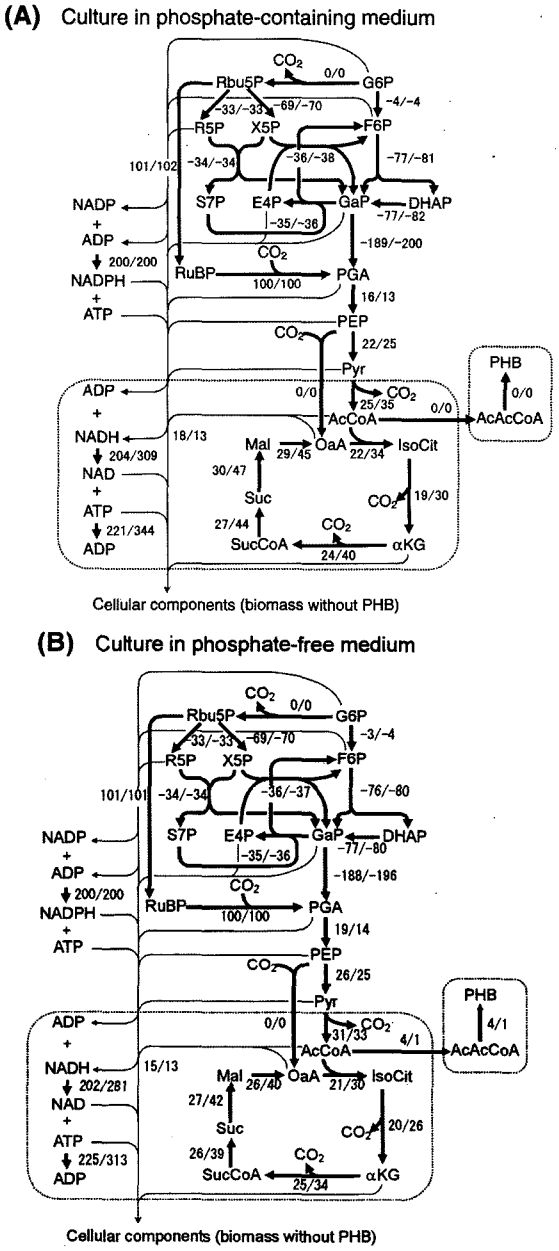

Fig. 5. Typical flux distributions of metabolic pathway in *Synechococcus* sp. MA19 cells cultivated at incident light intensity of 50 W/m^2. (A) Culture in phosphate-containing medium and (B) culture in phosphate-free medium. The flux values are normalized by the flux for CO_2 fixation by RuBisCO. The left- and right-hand numerals are the flux values calculated for culture times from 22 to 47 h and from 194.5 to 215 h (A), and culture times from 24 to 49 h and from 120 to 170 h (B).

Metabolic Flux Distributions in *Synechococcus* sp. MA19 Cells

Based on the metabolic network model and the measured experimental data, intracellular flux distributions

were calculated to evaluate the states of MA19 cells grown under the photoautotrophic conditions. A comparison of metabolic fluxes was made in the cultures using the media with and without phosphate (Figs. 3 and 4). Fig. 5 represents the typical flux distributions calculated from the data obtained in the cultures using the phosphate-containing medium (t = 22-47 and 194.5 -215 h), and from the cultures using the phosphate-free medium (t = 24-49 and 120-170 h), respectively. The numerical values indicating fluxes are normalized by the calculated flux value for CO_2 fixation by ribulose-1,5-bisphosphate carboxylase/oxygenase (RuBisCO), and the left and right-hand sides of figures show the fluxes during the respective culture times indicated.

In the culture with the phosphate-containing medium (Fig. 5(A)), the mean values of light energy absorbed by the cells were $E_C = 5.1 \times 10^6$ and 2.4×10^6 J h^{-1} kg^{-1} for t = 22-47 and 194.5-215 h, respectively. Concerning the flux distributions, the flux of biomass synthesis obviously decreased when the light energy absorbed by the cells reduced, which can be explained by a decrease in the fixation of CO_2 via RuBisCO activated by photo-irradiation. In the case of the phosphate-free medium (Fig. 5(B)), the mean values of light energy absorbed by the cells were $E_C = 3.1 \times 10^6$ and 1.5×10^6 J h^{-1} kg^{-1} for t = 24-49 and 120-170 h, respectively. A significant decrease in the flux of PHB synthesis was recognized at the lowered value of $E_C = 1.5 \times 10^6$ J h^{-1} kg^{-1}. With respect to the oxidative phosphorylation pathway, appreciable changes in the flux distributions were found between the early phase (t = 22-47 and 24-49 h) and the middle phase (t = 194.5-215 and 120-170 h) in both cultures using media with and without phosphate. From the results seen in Fig. 5(A) and (B), it was obvi ous that a decline in the E_C value led to the deteriorated potentials of biomass and PHB syntheses in the photoautotrophic culture of MA19 cells. The E_C value can be kept at a desirable level by regulating incident light intensity along with the change of cell concentration, which may offer a strategy for the maintenance of relatively high flux of PHB synthesis during the culture.

Estimation of Energy Efficiency Based on Metabolic Flux Analysis

To evaluate the efficiency of energy capture, the amounts of ATP and biomass (cellular components) syntheses were estimated based on the metabolic flux analysis. The flux distributions in the metabolic pathway were calculated in the different cultures of MA19 cells conducted under the examined conditions. The relative quantities of biomass formed and ATP synthesized, m_{cell} and n_{ATP} respectively, were defined as follows.

$$m_{cell} = (x_{26}XV\Delta t)M_{cell} \quad (9)$$

$$n_{ATP} = (x_4 + x_6 + 2x_{15} + x_{21} + 4x_{24} + 2x_{25})XV\Delta t \quad (10)$$

where x_{26} is the calculated flux value of biomass formation, x_4, x_6, x_{15}, x_{21}, x_{24} and x_{25} are the calculated flux values concerning ATP synthesis (Appendix B).

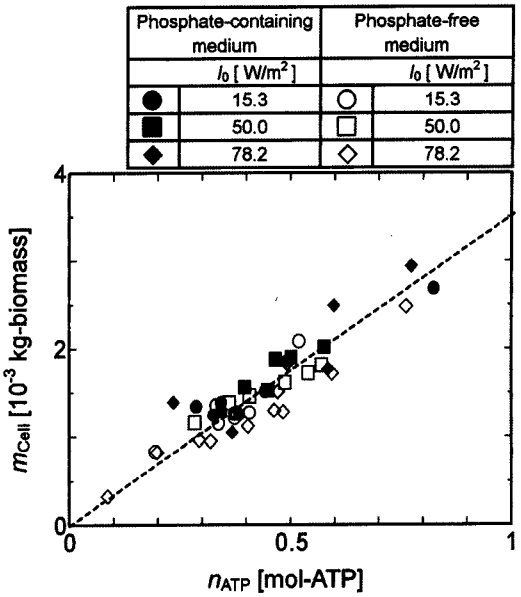

Fig. 6. Relationship between amounts of biomass and ATP synthesized in *Synechococcus* sp. MA19 cells cultivated under various conditions.

As shown in Fig. 6, a linear relationship was found between the values of m_{cell} and n_{ATP}, regardless of the culture conditions such as the incident light intensity and medium composition relating to PHB accumulation in MA19 cells, which indicates that the ATP synthesis would be a rate-limiting step in the growth of MA19 cells. The slope of the dotted line shown in Fig. 6 implies cell yield based on ATP, $Y_{ATP} = m_{cell}/n_{ATP}$. The value of Y_{ATP} was estimated as $Y_{ATP} = 3.5 \times 10^{-3}$ kg-biomass/mol-ATP (correlation coefficient: 0.93).

Using the data from the metabolic flux analysis, the energies converted from light to ATP and reducing poteintial (NADH + NADPH), E_{ATP} and E_{RED} respectively, were also calculated, as defined by the following equations.

$$E_{ATP} = (x_4 + x_6 + 2x_{15} + x_{21} + 4x_{24} + 2x_{25})(-\Delta G^{\circ}_{ATP}) \quad (11)$$

$$E_{RED} = n_e F\{(x_{17} + x_{20} + 2x_{22} + x_{23} + 0.101x_{26})(-\Delta E^{\circ}_{NADH}) + (x_4 + 2x_8 + 2x_{15} + x_{19})(-\Delta E^{\circ}_{NADPH})\} \quad (12)$$

where x_4, x_6, x_{15}, x_{21}, x_{24} and x_{25} are the calculated flux values for ATP synthesis, x_{17}, x_{20}, x_{22}, x_{23}, and x_{26} are those for NADH synthesis, and x_4, x_8, x_{15} and x_{19} are those for NADPH synthesis (Appendix B). In Eqs.(11) and (12), the value of $\Delta G^{\circ}_{ATP} = -2.93 \times 10^4$ J/mol, $n_e = 2$, $F = 9.65 \times 10^4$ C/mol, and ΔE°_{NADP} and $\Delta E^{\circ}_{NADPH} = -0.32$ V were adopted [19].

Figs. 7(A) and (B) represent the plots of E_{ATP} and E_{RED} values against the E_C value, respectively. The data obtained from the cultures with and without PHB synthesis were overlapped with each other in both cases of

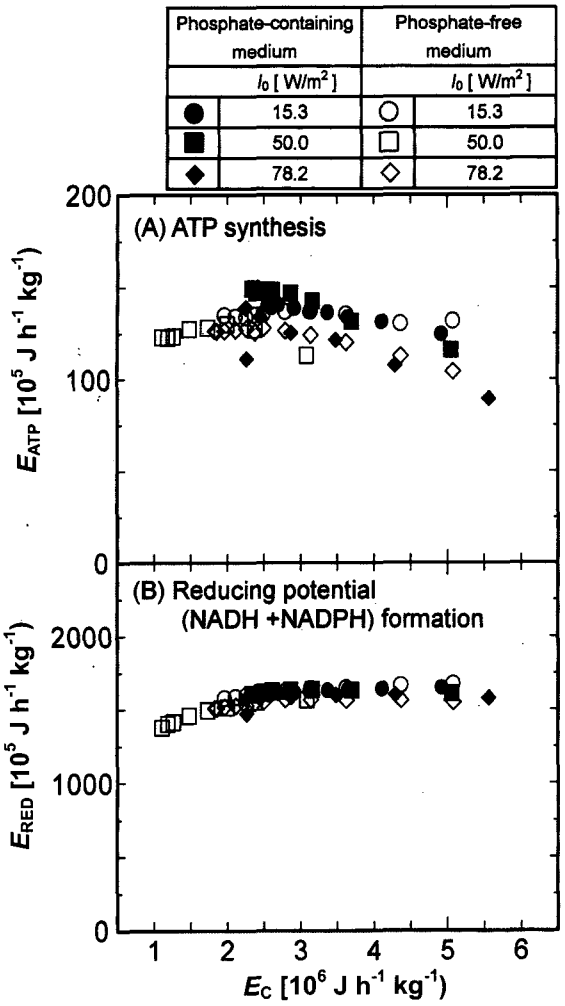

Fig. 7. Efficiencies of light energy conversion in *Synechococcus* sp. MA19 cells cultivated under various conditions. (A) Energy as ATP and (B) energy as reducing potential (NADH + NADPH) plotted against light energy absorbed by cells.

energies estimated as ATP (E_{ATP}) and reducing potential (E_{RED}). With respect to E_{ATP}, the values were maximized around E_C = 2.5-3.0 × 10^6 J h^{-1} kg^{-1}, whereas the flat profile of E_{RED} was obtained in the examined range of the energy absorbed by the cells. It is thus suggested that the light energy can be effectively utilized when the light intensity is regulated keeping the E_C value at 2.5-3.0 × 10^6 J h^{-1} kg^{-1}.

In conclusion, the cell yield based on ATP synthesis was estimated as 3.5 × 10^{-3} kg-biomass/mol-ATP, based on the metabolic flux analysis of MA19 cells grown under the photoautotrophic conditions. Under the examined conditions, the energy converted from light to ATP was kept relatively high in the vicinity of E_C = 2.5-3.0 × 10^6 J h^{-1} kg^{-1}, which will offer useful information to cultivate MA19 cells under a controlled light condition.

NOMENCLATURE

A	side area of flask receiving incident light [m^2]
a_{ij}	stoichiometric coefficient of metabolite i in reaction j [-]
CUR	CO_2 uptake rate [mol h^{-1} kg^{-1}]
E_C	light energy absorbed by cells [J h^{-1} kg^{-1}]
E_M	light energy absorbed in cell-free medium [J/h]
E_T	total light energy absorbed in cell suspension [J/h]
E_{ATP}	energy as ATP per unit weight of cell mass [J h^{-1} kg^{-1}]
E_{RED}	energy as reducing potential (NADH + NADPH) per unit weight of cell mass [J h^{-1} kg^{-1}]
F	Faraday's constant [C/mol]
i	metabolite [-]
I_0	incident light intensity [W/m^2]
j	metabolic reaction [-]
L	length of light pass [m]
M_{cell}	provisional molecular weight of cellular components (biomass without PHB) [kg/mol]
m_{cell}	amount of biomass synthesized [kg-biomass]
n_e	number of electron transferred [-]
n_{ATP}	amount of ATP synthesized [mol-ATP]
OER	O_2 evolution rate [mol h^{-1} kg^{-1}]
R_P	PHB content in cell mass [% (w/w)]
$\boldsymbol{r}$	vector of m-dimensional metabolite accumulation rate [mol h^{-1} kg^{-1}]
r_i	accumulation rate of metabolite i [mol h^{-1} kg^{-1}]
r_o	actual O_2 evolution rate [mol h^{-1} kg^{-1}]
$\boldsymbol{S}$	$m \times n$ matrix of stoichiometric coeffecient [-]
t	culture time [h]
V	volume of medium [m^3]
X	cell mass concentration [kg/m^3]
X_C	concentration of cellular components (biomass without PHB) [kg-biomass/m^3]
$\boldsymbol{x}$	n-dimensional flux vector [-]
x_j	flux through reaction j [mol h^{-1} kg^{-1}]
Y_{ATP}	cell yield based on ATP [kg-biomass/mol-ATP]
α	effective absorption coefficient of light [m^{-1}]
ΔG°_{ATP}	free energy change in reaction of ATP hydrolysis [J/mol]
ΔE°_{NADH}	potential change in oxidation of NADH [V]
ΔE°_{NADPH}	potential change in oxidation of NADPH [V]
φ	vector of measurement noise variance-covariance [-]

Appendix A. Metabolite *i* (*i* = 1-29) for Construction of Accumulation Rate Vector

1	ACACCOA	Acetoacetyl coenzyme A
2	ACCOA	Acetyl coenzyme A
3	αKG	α-Ketoglutarate
4	ATP	Adenosine 5'-triphosphate
5	BIOMAS	Cellular components (M_{cell} = 0.1 kg/mol for convenience)
6	CO_2	Carbon dioxide
7	DHAP	Dihydroxyacetone-phosphate

8	E4P	Erythrose-4-phosphate
9	F6P	Fructose-6-phosphate
10	FADH	Flavin adenine dinucleotide, reduced form
11	G6P	Glucose-6-phosphate
12	GAP	Glyceraldehyde-3-phosphate
13	ISOCIT	Isocitrate
14	MAL	Malate
15	NADH	Nicotinamide adenine dinucleotide, reduced form
16	NADPH	Nicotinamide adenine dinucleotide phosphate, reduced form
17	O_2	Oxygen
18	OAA	Oxaloacetate
19	PEP	Phosphoenolpyruvate
20	PGA	Phosphoglycerate
21	PHB	Poly-β-hydroxybutyrate
22	PYR	Pyruvate
23	R5P	Ribose-5-phosphate
24	RBU5P	Ribulose-5-phosphate
25	RUBP	Ribulose-1,5-bisphosphate
26	S7P	Sedoheptulose-7-phosphate
27	SUC	Succinate
28	SUCCOA	Succinyl coenzyme A
29	X5P	Xylulose-5-Phosphate

Appendix B. Metabolic Reaction *j* (*j* = 1-29)

Glycolysis (Embden-Meyerhof-Parnas pathway)

1 G6P = F6P
2 F6P + ATP = GAP + DHAP + ADP
3 DHAP = GAP
4 GAP + ADP + NADP= PGA + NADPH + ATP
5 PGA = PEP + H_2O
6 PEP + ADP = ATP + PYR

Anaplerotic reaction

7 PEP + CO_2 = OAA

Pentose phosphate

8 G6P + H_2O + 2 NADP = RBU5P + CO_2 + 2 NADPH
9 RBU5P = R5P
10 RBU5P = X5P
11 X5P + R5P = S7P + GAP
12 S7P + GAP = F6P + E4P
13 X5P + E4P = F6P + GAP
14 RBU5P + ATP = RUBP + ADP

Photophosphorylation

15 2 NADP + 2 ADP + 2 H_2O = 2 NADPH + 2 ATP + O_2

CO_2 fixed reaction

16 RUBP + CO_2 = 2 PGA

Tricarboxylic acid cycle

17 PYR + COA + NAD = ACCOA + CO_2 + NADH
18 ACCOA + OAA + H_2O = ISOCIT + COA
19 ISOCIT + NADP = αKG + NADPH + CO_2
20 αKG + COA + NAD = SUCCOA + CO_2 + NADH
21 SUCCOA + ADP = SUC + COA + ATP
22 SUC + H_2O + FAD = MAL + FADH
23 MAL + NAD = OAA + NADH

Oxidative phosphorylation (P/O = 2)

24 2 NADH + O_2 + 4 ADP = 2 H_2O + 4 ATP + 2 NAD
25 2 FADH + O_2 + 2 ADP = 2 H_2O + 2 ATP + 2 FAD

Biomass synthesis

26 0.193 PYR + 0.073 αKG + 0.092 OAA + 0.050 PGA + 0.0081 R5P + 0.39 ACCOA + 0.015 E4P + 0.061 PEP + 0.0114 GAP + 0.180 G6P + 0.064 F6P + 0.515 NO_3 + 1.050 ATP + 1.242 NADPH + 0.101 NAD = BIOMAS + 1.050 ADP + 1.242 NADP + 0.101 NADH

Unaccounted for ATP requirements

27 ATP = ADP

PHB synthesis pathway

28 2 ACCOA = ACACCOA + COA
29 ACACCOA + NADPH = PHB + COA + NADP

REFERENCES

[1] Campbell, J. III., S. E. Stevens Jr., and D. L. Balkwill (1982) Accumulation of poly-β-hydroxybutyrate in *Spirulina plantensis*. *J. Bacteriol.* 149: 361-363.
[2] Stal, L. J. (1992) Poly(hydroxyalkanoate) in cyanobacteria: an overview. *FEMS Microbiol. Rev.* 103: 169-180.
[3] Nishioka, M., K. Nakai, M. Miyake, Y. Asada, and M. Taya (2001) Production of poly-β-hydroxybutyrate by thermophilic cyanobacterium, *Synechococcus* sp. MA19, under phosphate-limited conditions. *Biotechnol. Lett.* 23: 1095-1099.
[4] Miyake, M., M. Erata, and Y. Asada (1996) A thermophilic cyanobacterium, *Synechococcus* sp. MA19, capable of accumulating poly-β-hydroxybutyrate. *J. Ferment. Bioeng.* 82: 512-514.
[5] Aiba, S. and M. Matsuoka (1979) Identification of metabolic model: citrate production from glucose by *Candia lipolytica*. *Biotechnol. Bioeng.* 21: 1373-1386.
[6] Vallino, J. J. and G. Stephanopoulos (1993) Metabolic flux distribution in *Corynebacterium glutamicum* during growth and lysine overproduction. *Biotechnol. Bioeng.* 41: 633-646.
[7] Shi, H., M. Shiraishi, and K. Shimizu (1997) Metabolic flux analysis of poly-(β-hydroxybutyric acid) in *Alcaligenes eutrophus* from various carbon sources. *J. Ferment. Bioeng.* 84: 579-587.
[8] Takiguchi, N., H. Shimizu, and S. Shioya (1997) An online physiological state recognition system for the lysine fermentation process based on a metabolic reaction model. *Biotechnol. Bioeng.* 55: 170-181.
[9] Hua, Q., P. C. Fu, C. Yang, and K. Shimizu (1998) Microaerobic lysine fermentation and metabolic flux analysis. *Biochem. Eng. J.* 2: 89-100.
[10] Yang, C., Q. Hua, and K. Shimizu (2000) Energetics and carbon metabolism during growth of microalgal cells un-

der photoautotrophic, mixotrophic and cyclic light-autotrophic/dark-heterotrophic conditions. *Biochem. Eng. J.* 6: 87-102.

[11] Yang, C., Q. Hua, and K. Shimizu (2002) Quantitative analysis of intracellular metabolic fluxes using GC-MS and two-dimensional NMR spectroscopy. *J. Biosci. Bioeng.* 93: 78-87.

[12] Rippka, R., J. Deruelles, J. B. Waterbury, M. Herdman, and R. Y. Stanier (1979) Genetic assignments, strain histories and properties of pure cultures of cyanobacteria. *J. Gen. Microbiol.* 111: 1-61.

[13] Hirata, S., J. Hata, M. Taya, and S. Tone (1997) Growth estimation of *Spirulina plantensis* by considering light distribution in photoautotrophic batch culture. *J. Chem. Eng. Jpn.* 30: 355-359.

[14] Hata, J., Q. Hua, C. Yang, K. Shimizu, and M. Taya (2000) Characterization of energy conversion based on metabolic flux analysis in mixotrophic liverwort cells, *Marchantia polymorpha*. *Biochem. Eng. J.* 6: 65-74.

[15] Vallino, J. J. and G. Stephanopoulos. (1990) Flux determination in cellular bioreaction networks: application to lysine fermentation. pp. 205-219 In: S. K. Sikdar, M. Bier, and P. Todd (eds.). *Frontiers in Bioprocessing*. CRC Press, Boca Raton, FL, USA.

[16] Stumpf, P. K. and E. E. Conn (1980) *The Biochemistry of Plants*. Vol. 2. pp. 1-27. Academic Press, New York, NY, USA.

[17] Holms, W. H. (1986) The central metabolic pathways of *Escherichia coli*: relationship between flux and control at a branch point, efficiencies of conversion to biomass, and excretion of acetate. *Curr. Topics Cell. Reg.* 28: 69-105.

[18] Ingraham, J. L., O. Maaloe, and F. C. Nedhardt (1983) *Growth of the Bacterial Cell*. pp. 87-173. Sinauer Associates, Sunderland, MA, USA.

[19] Rawn, J. D. (1989) *Biochemistry*. Neil Patterson Publishers, Burlington, NC, USA.

[Received March 10, 2002; accepted June 28, 2002]